


## Biomimetic Receptor | Hot Paper |

 Submerging a Biomimetic Metallo-Receptor in Water for Molecular Recognition: Micellar Incorporation or Water Solubilization? A Case StudySolène Collin,<sup>[a]</sup> Arnaud Parrot,<sup>[a]</sup> Lionel Marcelis,<sup>[b]</sup> Emilio Brunetti,<sup>[b, c]</sup> Ivan Jabin,<sup>[c]</sup> Gilles Bruylants,<sup>[b]</sup> Kristin Bartik,<sup>\*[b]</sup> and Olivia Reinaud<sup>\*[a]</sup>

**Abstract:** Molecular recognition in water is an important topic, but a challenging task due to the very competitive nature of the medium. The focus of this study is the comparison of two different strategies for the water solubilization of a biomimetic metallo-receptor based on a poly(imidazole) resorcinarene core. The first relies on a new synthetic path for the introduction of hydrophilic substituents on the receptor, at a remote distance from the coordination site. The second involves the incorporation of the organosoluble metallo-receptor into dodecylphosphocholine (DPC) micelles, which mimic the proteic surrounding of the active site of metallo-enzymes. The resorcinarene ligand can be transferred into water through both strategies, in which it binds

Zn<sup>II</sup> over a wide pH window. Quite surprisingly, very similar metal ion affinities, pH responses, and recognition properties were observed with both strategies. The systems behave as remarkable receptors for small organic anions in water at near-physiological pH. These results show that, provided the biomimetic site is well structured and presents a recognition pocket, the micellar environment has very little impact on either metal ion binding or guest hosting. Hence, micellar incorporation represents an easy alternative to difficult synthetic work, even for the binding of charged species (metal cations or anions), which opens new perspectives for molecular recognition in water, whether for sensing, transport, or catalysis.

## Introduction

The study of molecular recognition processes in water is a field of great interest, not only for the elaboration of efficient and selective sensors for environmental analyses or the development of green catalysts, but also for the elucidation of biological processes.<sup>[1]</sup> The major difficulties encountered in water, compared to organic solvents, stem from the intrinsic properties of this solvent.<sup>[2]</sup> Indeed, it provides a very competitive medium for electrostatic interactions, and particularly for direc-


tional H-bonding interactions. It is thus necessary to invoke other types of stabilizing effects in order to extract analytes from water. The hydrophobic effect<sup>[3]</sup> can be exploited for analytes that present an apolar component in their structure.<sup>[4,5]</sup> For highly polar compounds, such as small anions,<sup>[6,7]</sup> coordination to a metal cation<sup>[8–10]</sup> can provide an efficient means of shifting the equilibria towards the formation of a host-guest adduct, that is, a metal complex.<sup>[11]</sup> However, water is also a strong competitor in the case of metal coordination due to its good donor ability in its neutral form or as hydroxide. In Nature, and in particular in the case of proteins, this problem is circumvented<sup>[12]</sup> as the metallo active sites are generally associated with a well-defined hydrophobic cavity that also plays a major role in substrate recognition.

Inspired by this design, we are developing biomimetic cavity-based metal complexes as a tool for molecular recognition.<sup>[13]</sup> A common feature of these so-called “funnel” or “bowl” complexes is a hydrophobic cavity in the vicinity of a coordinated metal ion, with which it acts in synergy for guest binding. The funnel complexes, based on a flexible calix[6]arene core, have been shown to display remarkable recognition properties towards neutral guests, presenting both good donor ability for metal ion binding and good shape complementarity of the cone cavity (Figure 1, left).<sup>[14–17]</sup> Surprisingly, most of these complexes have proven to be resistant to anion binding, making them unusually selective.<sup>[18]</sup> This has been attributed to electrostatic repulsion by the oxygen-rich narrow

[a] Dr. S. Collin, Dr. A. Parrot, Prof. O. Reinaud  
Laboratory of Pharmacological and Toxicological Chemistry  
and Biochemistry  
Université Paris Descartes  
45, rue des Saints-Pères, 75006 Paris (France)  
E-mail: olivia.reinaud@parisdescartes.fr

[b] Dr. L. Marcelis, Dr. E. Brunetti, Prof. G. Bruylants, Prof. K. Bartik  
Engineering of Molecular Nanosystems  
Université Libre de Bruxelles  
Avenue F. D. Roosevelt 50, CP165/64, 1050 Brussels (Belgium)  
E-mail: kbartik@ulb.ac.be

[c] Dr. E. Brunetti, Prof. I. Jabin  
Laboratory of Organic Chemistry  
Université Libre de Bruxelles  
Avenue F. D. Roosevelt 50, CP160/06, 1050 Brussels (Belgium)

 Supporting information and the ORCID identification number(s) for the author(s) of this article can be found under:  
<https://doi.org/10.1002/chem.201804768>.

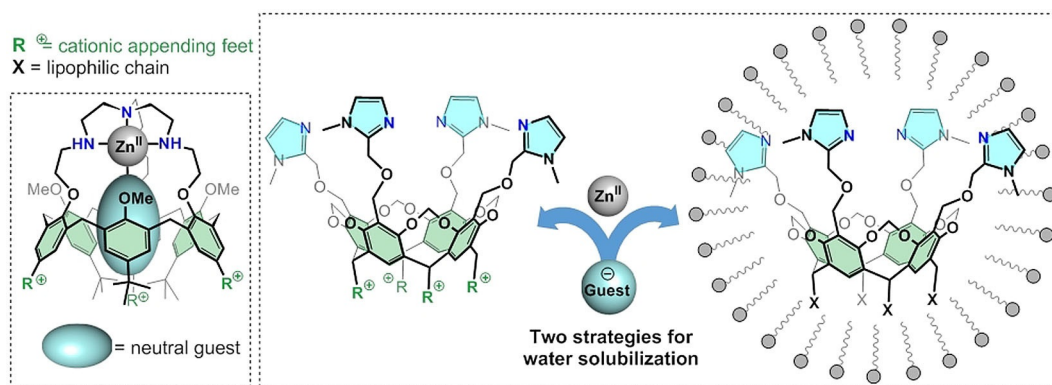


**Figure 1.** Left: A water-soluble funnel complex. Right: two strategies for water solubilization of a resorcinarene-based Zn<sup>II</sup> receptor, the subject of this article.

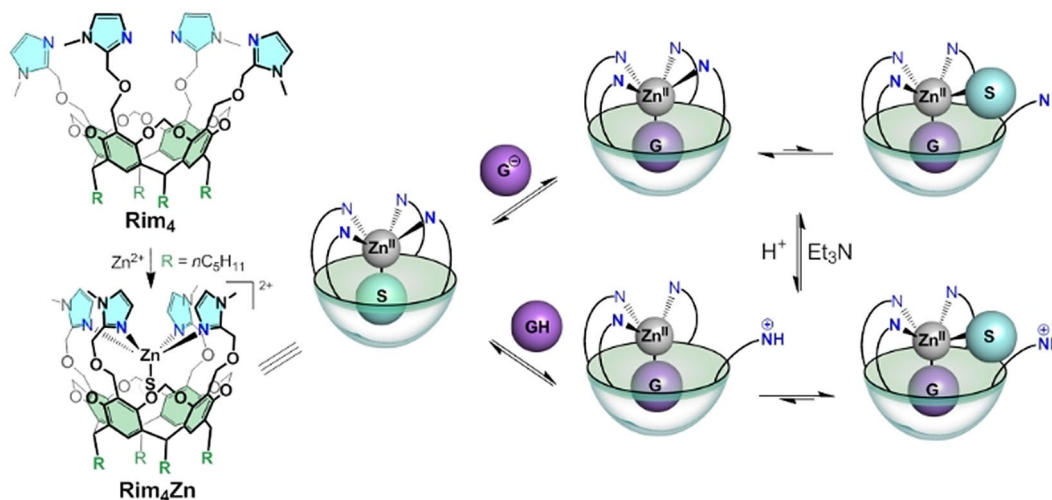
rim as a second coordination sphere. In contrast, rigid bowl-shaped resorcinarene-based metal complexes, offering a very different second coordination sphere and shape, display strong affinity towards small anionic guests.<sup>[19]</sup>

Our most recently described bowl complex, based on the new ligand **Rim<sub>4</sub>**,<sup>[20]</sup> is depicted in Scheme 1. In this system, the resorcinarene is functionalized at its large rim with four imidazole arms, three of which firmly hold the Zn<sup>II</sup> ion at the entrance of the bowl-shaped cavity, whereas the fourth is hemilabile. We have shown that this hemilabile arm assists the deprotonation of a neutral guest molecule, which can then bind as an anion to the metal center. It has also been shown to promote the selective base-catalyzed hydration of acetonitrile to afford acetamide, which we term “a third degree of biomimetism”.<sup>[20]</sup> In our quest towards more biomimetism, the following aspects have been considered: i) the solvent for the natural systems, that is, enzymes, is water; and ii) in soluble enzymes, the active site is surrounded by a large proteic structure, mostly hydrophobic at its core, whereas a polar surface ensures its solubility in water.

To address this new aspect of biomimetism, two different strategies have been considered for water-solubilization of the **Rim<sub>4</sub>Zn<sup>II</sup>** system. The first strategy involves the incorporation of

hydrophilic moieties into the macrocyclic structure. This requires careful synthetic design to avoid interaction between the hydrophilic moieties and the metal ion and often necessitates laborious synthetic work. Such a strategy has previously been successfully applied to various funnel complexes, as illustrated by tris(imidazole)Zn<sup>II</sup>-based and trenCu<sup>II</sup>-based calix[6]arene systems, which serve as selective receptors for lipophilic primary amines in water.<sup>[21,22]</sup> The second strategy relies on incorporation of an organo-soluble metal complex into micelles. This has been previously exemplified for a metallo-receptor with a uranyl-salophen complex for anion binding.<sup>[23,24]</sup> More recently, we have reported the successful incorporation of a calix[6]arene Zn<sup>II</sup> funnel complex into DPC micelles and have shown that the system retains its hosting properties towards amines at physiological pH. However, none of these funnel complexes are capable of recognizing anions, even lipophilic ones.<sup>[25]</sup>

Here, we report a study that compares two different strategies for water-solubilization of a resorcinarene-based metallo-receptor (Figure 1, right) for the recognition of small organic guests that are bound in their anionic form (Figure 1, right): direct solubilization of the ligand in water, which will then surround the metallo-receptor, or encapsulation into a zwitterion-



**Scheme 1.** Schematic structure and general host–guest behavior of complex **Rim<sub>4</sub>Zn<sup>II</sup>** in MeCN. G<sup>(-)</sup> denotes an anionic guest ligand and S denotes a solvent or water molecule.

ic micelle that will mimic the hydrophobic environment provided by the proteic backbone of natural systems.

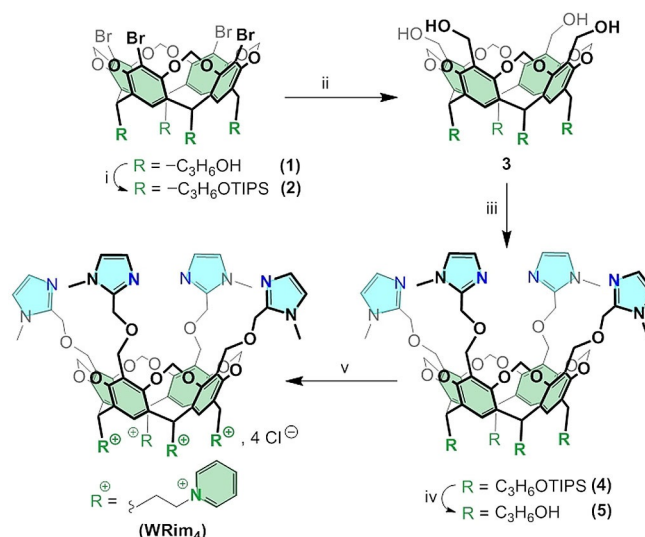
## Results and Discussion

### Synthesis of the water-soluble ligand WRim<sub>4</sub>

We have recently described a strategy for transforming an organo-soluble ligand based on a resorcinarene macrocycle bearing three imidazole groups (so-called Rim<sub>3</sub>)<sup>[26]</sup> into a water-soluble version through the introduction of quaternary ammonium groups as "feet".<sup>[27]</sup> The synthesis of WRim<sub>4</sub> followed a similar strategy (Scheme 2), but using pyridinium moieties as water-solubilizing feet, according to a procedure adapted from that previously reported by Rebek et al. for deep cavitands.<sup>[28]</sup>

The tetrabromo derivative **1** was obtained according to a previously reported route, in three steps from resorcinol.<sup>[29]</sup> After protection of the OH groups as silyl ethers, the resulting compound **2** was treated with *n*-butyllithium and paraformaldehyde to provide the corresponding tetra(alcohol) derivative **3**. The four imidazole groups were grafted onto the large rim using 2-chloromethyl-1-methyl-1*H*-imidazole with NaH to give compound **4**. Deprotection of the OH groups afforded product **5**, which was then reacted with chloromethylsulfonate (MsCl) and heated in pyridine to afford the target compound WRim<sub>4</sub> as its chloride salt. Its <sup>1</sup>H NMR spectra in CD<sub>3</sub>OD and D<sub>2</sub>O are displayed in Figure 2 and compared to that of Rim<sub>4</sub> in CDCl<sub>3</sub>.

As for the Rim<sub>4</sub> parent system in CDCl<sub>3</sub>, the <sup>1</sup>H NMR spectra of WRim<sub>4</sub> feature sharp and well-defined peaks in CD<sub>3</sub>OD as



**Scheme 2.** Synthesis of the water-soluble ligand WRim<sub>4</sub>. (i) TIPS-Cl, imidazole, DMF, 82%; (ii) *n*BuLi, paraformaldehyde, THF, -78 °C then rt, 45%; (iii) *N*-methylchloromethylimidazolium hydrochloride, NaH, DMF, 0 °C then rt; (iv) TFA, THF/H<sub>2</sub>O (1:1), 93% overall yield from **3**; (v) MsCl, pyridine, rt then 100 °C, 60%.

well as in D<sub>2</sub>O, consistent with a C<sub>4v</sub>-symmetrical structure (Figure 2). Comparison of the spectra in different solvents gives some insights into the relative environments of the protons. Several features can be discerned: all imidazole peaks display very similar  $\delta$  values (between 6.8 and 7.1 ppm, peaks labeled a and b). In contrast, the aromatic protons of the resorcinarene structure (labeled h) give rise to signals at very different

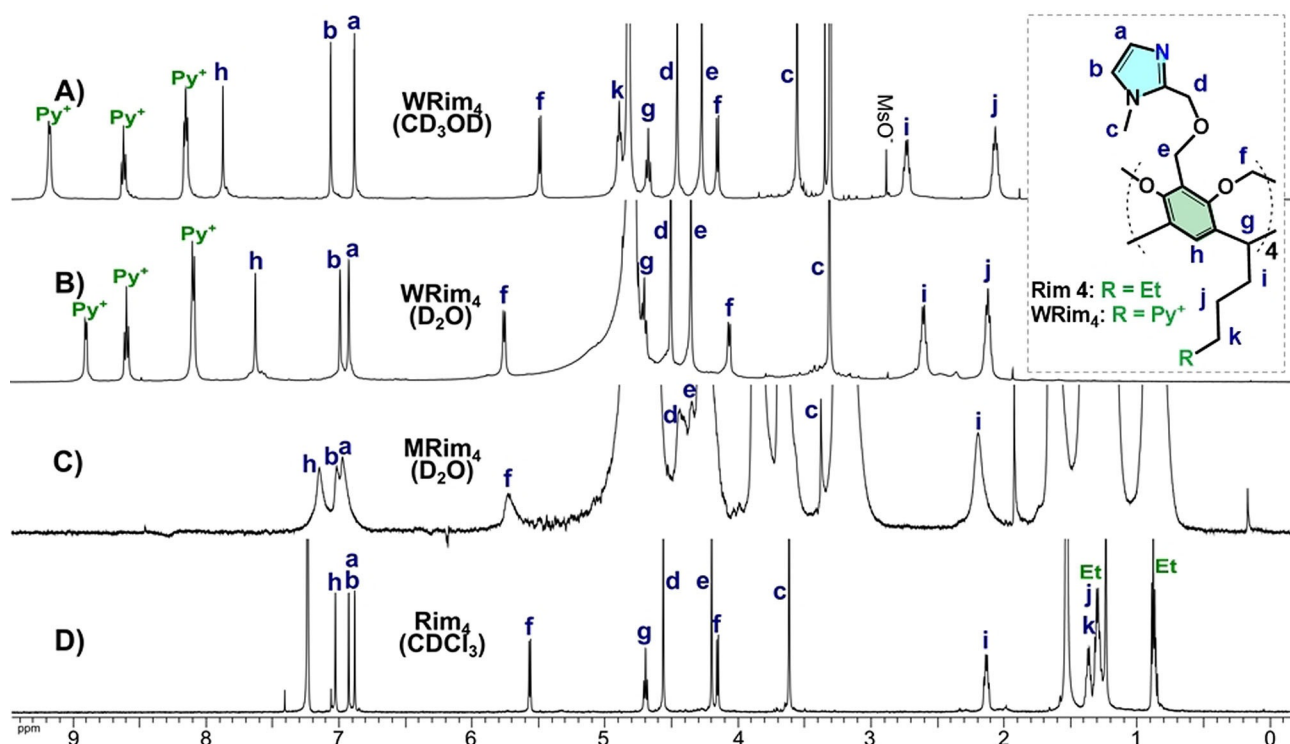


**Figure 2.** <sup>1</sup>H NMR spectra of Rim<sub>4</sub> systems in different media. From top to bottom: A) WRim<sub>4</sub> in CD<sub>3</sub>OD (500 MHz); B) WRim<sub>4</sub> in water (4 mm, pD 7.4, 500 MHz); C) MRim<sub>4</sub> in water (0.5 mm, pD 7.4, 20 mM DPC, 600 MHz); D) Rim<sub>4</sub> in CDCl<sub>3</sub> (600 MHz).

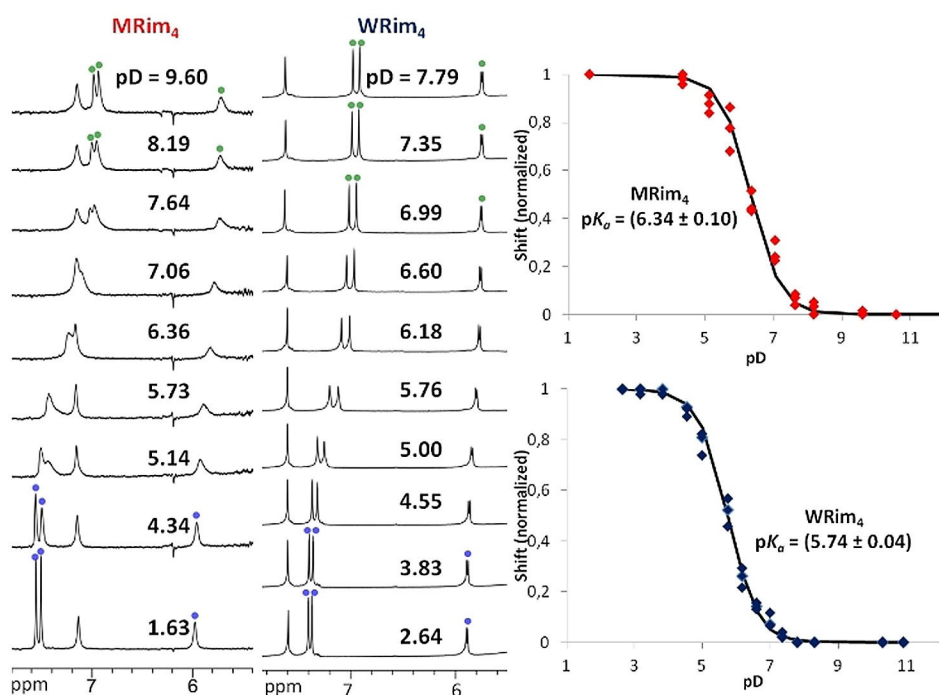


**Figure 3.** Evolution of the  $^1\text{H}$  NMR spectra of **MRim**<sub>4</sub> (0.5 mM, 20 mM DPC, left) and **WRim**<sub>4</sub> (2.5 mM, right) in  $\text{D}_2\text{O}$  as a function of pD (the full spectra are displayed in Figures S5 and S6). From acidic to basic conditions: tetraprotonated ligand (blue dots), the fully deprotonated ligand (green dots), and mixtures of protonated products between the pH extremes. The highlighted peaks correspond to, from left to right:  $\text{H}_b$  and  $\text{H}_a$  (imidazoles) and  $\text{H}_f$  (methylene bridges). The peak that does not shift with pH corresponds to the aromatic proton of the resorcinol units ( $\text{H}_r$ , see assignments in Figure 2). Right: normalized variations with pH of the chemical shifts of the dotted signals.

$\delta$  values, emphasizing the different environments provided by the solvents. Varying the pD from 2 to 11 led to shifts of the resonances corresponding to the imidazole arms due to different protonation states (Figure 3 and Figure S5 in the Supporting Information). As for the previously reported **WRim**<sub>3</sub> ligand, **WRim**<sub>4</sub> is fully protonated at pD < 3.8, and undergoes progressive deprotonation up to pD 7. At pD > 7, the NMR spectra showed no further change, consistent with deprotonation of all four imidazole donors. From the displacement of the chemical shifts according to pD, an average  $\text{p}K_a$  of 5.7 was determined for the four imidazole arms.

### Incorporation of **Rim**<sub>4</sub> into micelles

We recently described a very efficient means of incorporating a macrocyclic cationic metallo-receptor into micelles.<sup>[25]</sup> The receptor, a calix[6]arene-based  $\text{Zn}^{\text{II}}$  complex,<sup>[30]</sup> was successfully incorporated into dodecylphosphocholine (DPC) micelles, and the incorporated complex was observed to be stable over a wide pH range. We have now tested the same strategy with **Rim**<sub>4</sub>. Due to its insolubility in water as a neutral compound, it was incorporated into the micelles at low pH, at which it is in its protonated form.

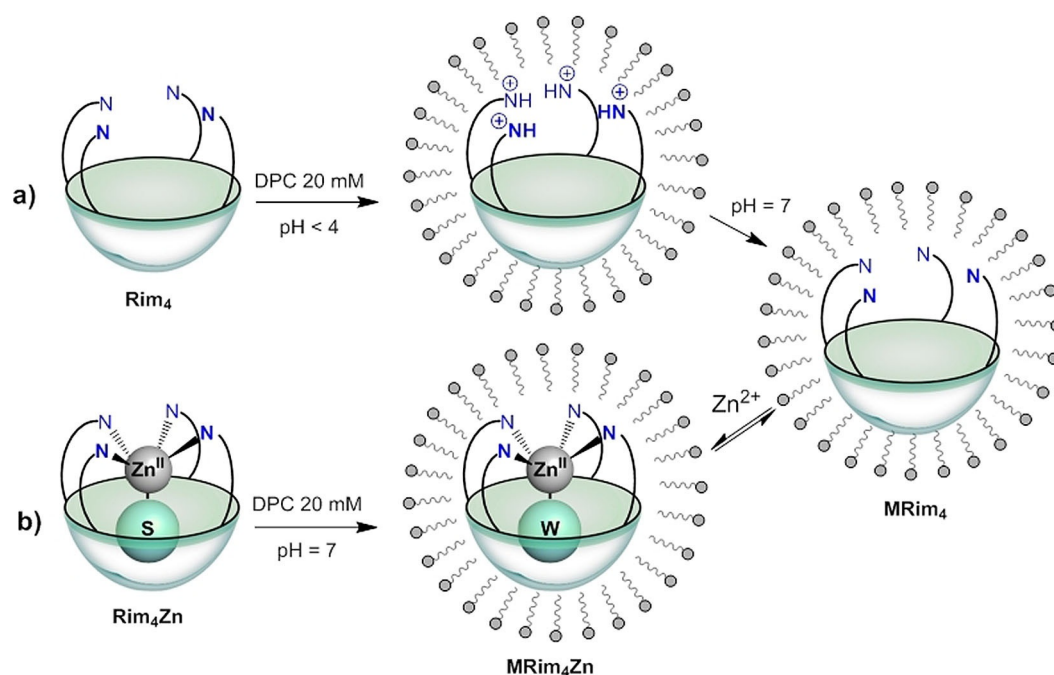
The corresponding NMR spectrum confirmed its solubilization in a fully protonated state. Once incorporated, the ligand remains inside the micelles at neutral and high pH, at which it is in its basic form (Figure 2c). A  $^1\text{H}$  NMR study at variable pH revealed that it remains fully protonated at up to pD  $\approx$  4, and

undergoes complete deprotonation at pD 8 (Figure 3 and Figure S6). The average  $\text{p}K_a$  of the imidazole arms of **MRim**<sub>4</sub> is 6.3, which represents a shift of 0.6 pH units compared with **WRim**<sub>4</sub>.

### $\text{Zn}^{\text{II}}$ complexation by **WRim**<sub>4</sub> and **MRim**<sub>4</sub>

The  $\text{Zn}^{\text{II}}$  complexes were readily obtained upon addition of one equivalent of  $\text{Zn}^{\text{II}}$  to millimolar solutions of either **WRim**<sub>4</sub> or **MRim**<sub>4</sub> in water at neutral pH. The **Rim**<sub>4</sub> $\text{Zn}^{\text{II}}$  complex could also be directly and efficiently incorporated into DPC micelles at neutral pH (Scheme 3), and it gave rise to an NMR signature identical to that of **MRim**<sub>4</sub> at neutral pH after the addition of  $\text{Zn}^{\text{II}}$ . DOSY spectra recorded for the **MRim**<sub>4</sub> $\text{Zn}^{\text{II}}$  system clearly showed the same diffusion coefficient for the surfactant and receptor (Figure S10), proving the incorporation of the ligand. The stabilities of the two **Rim**<sub>4</sub> $\text{Zn}^{\text{II}}$  systems were monitored as a function of pD by  $^1\text{H}$  NMR spectroscopy, and the spectra are presented in Figure 4. At low pD (< 4), the NMR signature corresponds to the protonated ligand, which indicates that zinc is not coordinated. As the pD is raised, the resonances of the imidazole arms start to shift upfield, indicative of formation of the  $\text{Zn}^{\text{II}}$  complex. At intermediate pD (6–8), the spectra indicate full complexation of  $\text{Zn}^{\text{II}}$ . At high pD (> 8), decomplexation starts to occur, as indicated by the emergence of new peaks in the aromatic region attributable to the free ligand, most probably associated with the formation of zinc hydroxide.<sup>[31]</sup>

The complexes are stable over wide pD ranges. For **WRim**<sub>4</sub> $\text{Zn}^{\text{II}}$  (2.5 mM), the 50% stability window is 4.9–8.7,



**Scheme 3.** Two pathways for obtaining  $\text{MRim}_4\text{Zn}^{\text{II}}$ . a) Incorporation of the ligand into DPC micelles at low pH followed by neutralization of the medium and  $\text{Zn}^{\text{II}}$  complexation; b) direct incorporation of the isolated organo-soluble complex at pH 7. S denotes a molecule of organic solvent; W denotes  $\text{H}_2\text{O}$  or  $\text{HO}^-$ .

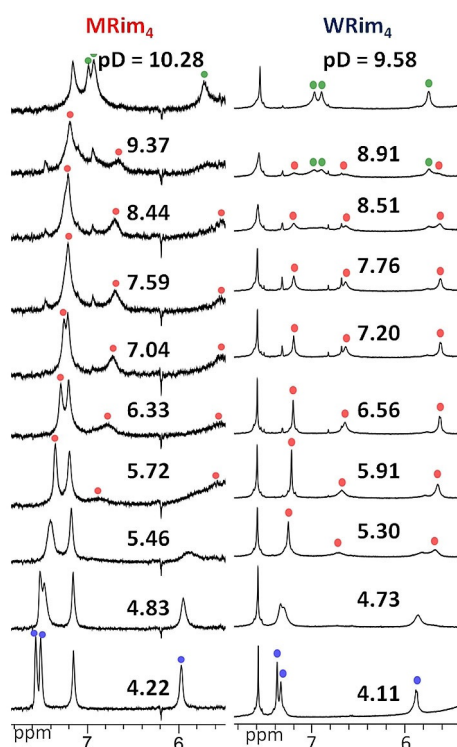


**Figure 4.** Evolution of the  $^1\text{H}$  NMR spectra of  $\text{MRim}_4$  (0.5 mM, left) and  $\text{WRim}_4$  (3.5 mM, right) in  $\text{D}_2\text{O}$  as a function of pD in the presence of 1 equivalent of  $\text{Zn}^{\text{II}}$  (the full spectra are displayed in Figures S8 and S11). From basic to acidic conditions: the neutral ligand (green dots), the zinc complex (red dots), the fully protonated ligand (blue dots). The highlighted peaks correspond to, from left to right:  $\text{H}_i$  and  $\text{H}_a$  (imidazoles) and  $\text{H}_f$  (methylene bridges). The unmarked peak, which does not shift, corresponds to the aromatic proton of the resorcinol units ( $\text{H}_b$ , see assignments in Figure 2). Note: in the 7.6–9.4 pH window, the signal of the aromatic proton of  $\text{MRim}_4$  overlaps with an imidazole peak.

whereas for  $\text{MRim}_4\text{Zn}^{\text{II}}$  (0.5 mM complex; 20 mM DPC) it is 5.6–9.8 (see Figures S8–S11). The pD window of stability observed for the micellar system spans slightly more basic values, consistent with the slightly higher  $\text{pK}_a$  value of the free ligand when incorporated into the micelles (see Table 1). Due to the multiple equilibria, the NMR studies did not allow identification of the protonation state of the guest (water or hydroxide), nor the possible protonation of one imidazole arm of the Zn complexes, as previously evidenced in MeCN (see above).

The binding constants for  $\text{Zn}^{\text{II}}$  at pH 7 were measured by isothermal titration calorimetry (ITC; Figures S9 and S12) and the corresponding thermodynamic parameters are reported in Table 1, together with those previously reported for  $\text{Rim}_4$  in acetonitrile<sup>[20]</sup> for comparison purposes.

In water, the binding constants of  $\text{Zn}^{2+}$  to  $\text{WRim}_4$  and  $\text{MRim}_4$  are surprisingly similar ( $K'_{\text{Zn}}$  ca.  $10^4 \text{ M}^{-1}$ ), with only small differences in the enthalpic and entropic components, in spite of the very different micro-environments surrounding the re-

**Table 1.** Binding constants and associated enthalpic and entropic parameters for  $\text{Zn}^{\text{II}}$  complexation by  $\text{Rim}_4$  in MeCN, and by  $\text{WRim}_4$  and  $\text{MRim}_4$  in water at pH 7. The values were determined by ITC of the ligands (0.25 mM and 0.5 mM) with a solution of  $\text{Zn}^{\text{II}}$  buffered by HEPES (100 mM and 50 mM) for  $\text{WRim}_4$  and  $\text{MRim}_4$ , respectively (see the Supporting Information and ref. [20] for data for  $\text{Rim}_4$ ).

Parameters	$\text{Rim}_4$	$\text{MRim}_4$	$\text{WRim}_4$
$K'_{\text{Zn}} (\text{M}^{-1})$	$(6 \pm 2) \times 10^5$	$(3 \pm 1) \times 10^4$	$(2 \pm 1) \times 10^4$
$\Delta H^{\circ}_{\text{Zn}} (\text{kJ mol}^{-1})$	$-70 \pm 7$	$-8.5 \pm 2$	$-11 \pm 3$
$\Delta S^{\circ}_{\text{Zn}} (\text{JK}^{-1} \text{mol}^{-1})$	$-100 \pm 23$	$60 \pm 10$	$50 \pm 15$
pD stability (50%)	— <sup>[a]</sup>	5.6–9.8	4.9–8.6

[a] In this case, the solvent was  $\text{CH}_3\text{CN}$ .

sorcinarene-based ligands. The  $K'_{Zn}$  values measured in water are only one order of magnitude lower than that measured in MeCN with **Rim<sub>4</sub>**, despite the stronger solvation of the metal ion. The stronger competition with the water solvent as a ligand compared to MeCN is well reflected in the enthalpic contribution,  $\Delta H'^{\circ}_{Zn}$ , which is much more favorable in MeCN than in water ( $-70$  vs. ca.  $-10$  kJ mol<sup>-1</sup>). The entropic component,  $\Delta S'^{\circ}_{Zn}$ , is positive for the systems in water, in contrast to what is observed in MeCN, in which it is negative ( $-100$  JK<sup>-1</sup> mol<sup>-1</sup>). The loss of entropy observed for the system in MeCN is a consequence of the more ordered state of the ligand when the metal complex is formed, since the imidazole arms are no longer able to freely move around. The positive  $\Delta S'^{\circ}_{Zn}$  values observed in water suggest that the desolvation of zinc and the related release of water molecules are entropically decisive. Moreover, in the case of **WRim<sub>4</sub>**, the hydrophobic effect minimizes ligand exposure to water when folding and wrapping around the Zn<sup>II</sup> ion. In micelles, a local solvophobic effect due to interpenetration of the lipophilic chain of the surfactant and the opened, unfolded bowl-shaped cavity of free **Rim<sub>4</sub>** might be responsible for the relatively high value of  $\Delta S'^{\circ}_{Zn}$  ( $+60$  JK<sup>-1</sup> mol<sup>-1</sup>). This study clearly evidences that, whereas in organic solvents Zn<sup>II</sup> coordination is enthalpically

driven, in water, the entropic contribution to  $\Delta G^{\circ}$  is dominant in both cases, with the presence of micelles having surprisingly little impact.

## Host-guest studies

### Carboxylates

We previously showed that, in MeCN, the **Rim<sub>4</sub>Zn<sup>II</sup>** complex can bind one equivalent of acetate in the *endo* position with high affinity. We have now carried out a comparative study with **WRim<sub>4</sub>** and **MRim<sub>4</sub>** to ascertain whether the micro-environment around the metal complex has an impact on the hosting properties of the Zn<sup>II</sup> complex. Titrations of **MRim<sub>4</sub>Zn<sup>II</sup>** and **WRim<sub>4</sub>Zn<sup>II</sup>** with sodium acetate at pD 7.4 were monitored by <sup>1</sup>H NMR spectroscopy (Figure 5). The spectra clearly showed the emergence of new signals at  $\delta \approx -2.4$  ppm, consistent with inclusion of the acetate ion in the bowl-shaped cavity. The presence of two signals in the high-field region, associated with two sets of three signals in the aromatic region (one for the macrocycle and two for imidazole moieties), is likely due to the co-existence of a solvated form of the host-guest system, in which a water ligand replaces one imidazole arm (see the structures displayed in Figure 5), as seen with **Rim<sub>4</sub>Zn<sup>II</sup>** in

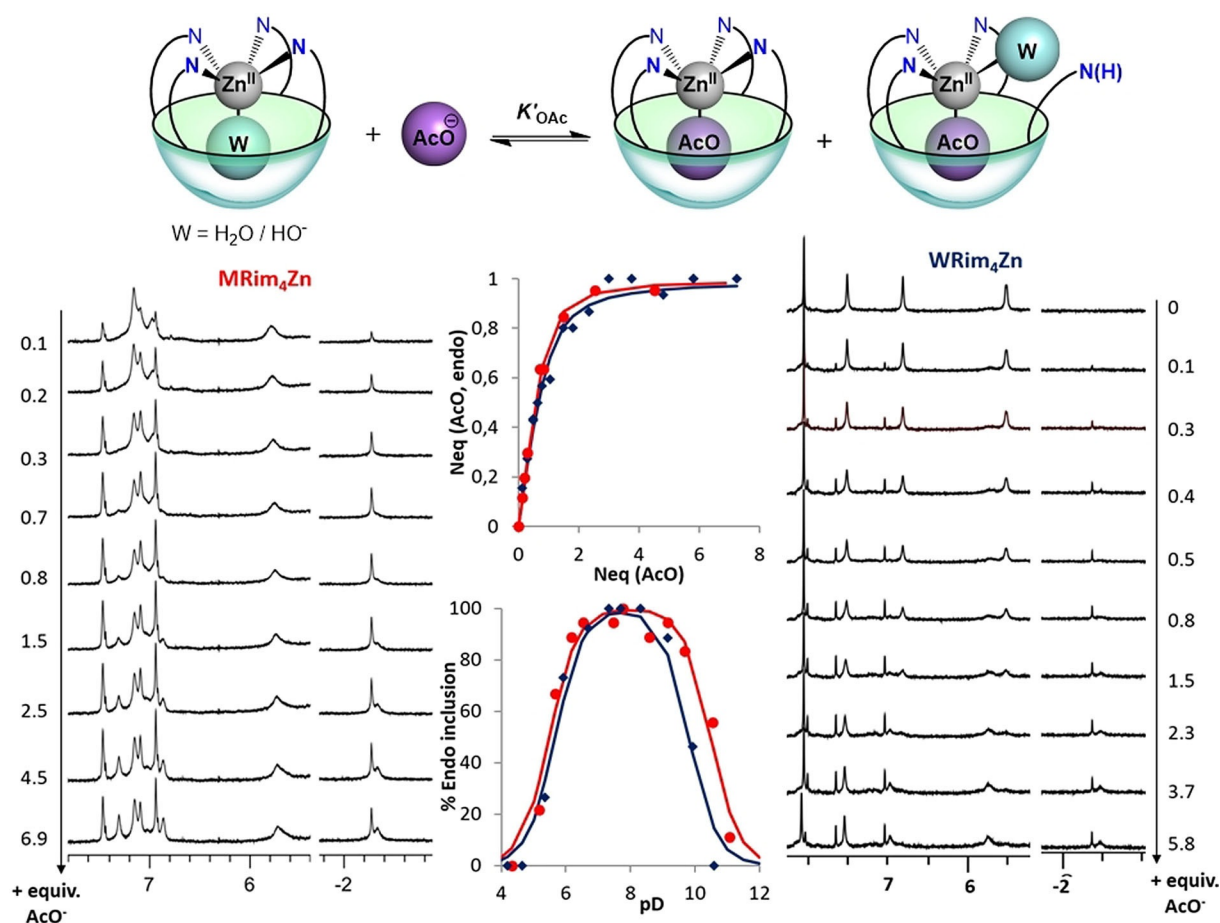


**Figure 5.** Acetate binding to **WRim<sub>4</sub>Zn<sup>II</sup>** and **MRim<sub>4</sub>Zn<sup>II</sup>** in water (W denotes a water or hydroxide ligand). Left and right: portions of the <sup>1</sup>H NMR spectra recorded in D<sub>2</sub>O at pD 7.4 during the titrations. Conditions: **WRim<sub>4</sub>Zn<sup>II</sup>** 0.7 mM in 100 mM HEPES buffer (300 K, 500 MHz); **MRim<sub>4</sub>Zn<sup>II</sup>** 0.5 mM, DPC 20 mM in HEPES 50 mM (298 K, 600 MHz). Center: fitting for 1:1 binding constants at pD 7.4 and pD stability window of the acetate complexes, as measured by integration of the peaks of the *endo*-bound acetate at  $\delta \approx -2.3$  ppm (see Figures S17–S19 for the corresponding complete NMR spectra).

**Table 2.** Data for host–guest properties of different **Rim<sub>4</sub>**-based Zn<sup>II</sup> complexes. For **MRim<sub>4</sub>** and **WRim<sub>4</sub>**, the binding constants were determined by <sup>1</sup>H NMR spectroscopy at pD 7.4 for acetate and at pD 8.4 for acetamide, and at pH 7 by ITC for acetylacetone (see the Supporting Information). The pD windows (given for 50% existence) were determined by <sup>1</sup>H NMR. For data for **Rim<sub>4</sub>**, see ref. [20].

Guest	Acetate			Acetylacetone			Acetamide		
	CIS <sup>[a]</sup> [ppm]	pD window (50%)	<i>K'</i> <sub>pH7.4</sub> [M <sup>-1</sup> ]	CIS <sup>[b]</sup> [ppm]	pD window (50%)	<i>K'</i> <sub>pH7</sub> [M <sup>-1</sup> ]	CIS <sup>[b]</sup> [ppm]	pD window (50%)	<i>K'</i> <sub>pH8.4</sub> [M <sup>-1</sup> ]
<b>MRim<sub>4</sub></b>	-4.2	5.5–10.5	2.2(±0.5) × 10 <sup>4</sup>	-4.5	5.7–11.2	2.8(±0.7) × 10 <sup>4</sup>	-4.3	7.9–nd	7(±1) × 10 <sup>2</sup>
<b>WRim<sub>4</sub></b>	-4.3	5.7–9.8	8.2(±1.0) × 10 <sup>3</sup>	-4.6	5.8–10.3	2.4(±0.7) × 10 <sup>4</sup>	-4.4	7.5–10.2	4(±1) × 10 <sup>2</sup>
<b>Rim<sub>4</sub></b>	-4.4	- <sup>[c]</sup>	> 10 <sup>4</sup>	-4.1	- <sup>[c]</sup>	> 10 <sup>4</sup>	-4.2	- <sup>[c]</sup>	1.2(±0.5) × 10 <sup>3</sup>

[a] The reference  $\delta$  shift for the free guest corresponds to acetate in water and acetic acid in MeCN. The CIS value corresponds to an average value of the two high-field peaks. [b] The reference  $\delta$  shift for the free guest corresponds to its neutral state. [c] In this case, the solvent was CH<sub>3</sub>CN.

MeCN solutions containing water. The corresponding *K'*<sub>OAc</sub> values, estimated by integration of the NMR signals for both systems, are very similar (1–2 × 10<sup>4</sup> M<sup>-1</sup>; see Figure 5 and Table 2). This suggests that the environment has little influence on the *endo* coordination of acetate, and this can be attributed to the presence of the bowl-shaped structure that surrounds the guest. Varying the pD revealed an optimal value of 7.4 for acetate binding in both systems (Figure 5). At high pD, the stability window is increased by ca. 1 pD unit compared to that for the metallo-receptor in the absence of the guest, with a significant advantage for the micellar system (10.5 vs. 9.8 for 50% complexation; see Tables 1 and 2).

The effect of the carboxylate length on coordination was also investigated. Addition of formate triggered a change in the NMR signature of **MRim<sub>4</sub>Zn<sup>II</sup>** consistent with its coordination, most likely in the *endo* position in view of its size and its behavior with **Rim<sub>4</sub>Zn<sup>II</sup>** in MeCN (*K'*<sub>HCO<sub>2</sub></sub> = 5 × 10<sup>2</sup> M<sup>-1</sup>). However, no coordination was seen with **WRim<sub>4</sub>** under similar experimental conditions, which may be attributed to the high solvation and small size of formate, making it not optimal for cavity filling. With the larger propionate anion, no modification of the NMR spectra was observed for either system with the addition of up to 50 equivalents, which highlights the selectivity of these systems.

### Acetylacetone

Titration of the **WRim<sub>4</sub>Zn<sup>II</sup>** and **MRim<sub>4</sub>Zn<sup>II</sup>** complexes with acetylacetone at pH 7.4 were monitored by <sup>1</sup>H NMR spectroscopy. Quantitative formation of the corresponding host–guest adducts was observed, with binding constants in excess of 10<sup>4</sup> M<sup>-1</sup>. The complexes were characterized by shifts of the peaks due to the imidazole arms and the emergence of new resonances at  $\delta$  = -2.35 and -2.20 ppm for **WRim<sub>4</sub>Zn<sup>II</sup>** and **MRim<sub>4</sub>Zn<sup>II</sup>**, respectively, consistent with the inclusion of a methyl group in the resorcinarene cavity. The NMR signatures and complexation-induced shift (CIS) values are very similar to those previously reported for **Rim<sub>4</sub>Zn<sup>II</sup>** in MeCN in the presence of acetylacetone and triethylamine (Table 2).<sup>[20]</sup> This indicates that, in water at pH 7, as in MeCN, acetylacetone is strongly bound to the metal ion as a result of its deprotonation, which leads to the bidentate anionic ligand, acetylacetonate, and concomitant displacement of one imidazole arm. In this complex, one guest methyl group resides in the *endo* position and

the other resides in an *exo* position, exposed to the solvent (see the structures displayed in Figure 6). The binding site of the receptor is thus expandable, as previously observed for **Rim<sub>3</sub>**.<sup>[19]</sup> The presence of only two resonances for the coordinating imidazole moieties in the aromatic region indicates that the imidazole arms are flipping quickly (relative to the NMR chemical shift time scale) from a coordinated state to an uncoordinated one, as previously observed for **Rim<sub>4</sub>** in MeCN.

Varying the pH evidenced efficient recognition over wide pH windows for both systems. With **WRim<sub>4</sub>** (0.5 mM), the 50% stability window for the acetylacetonate Zn<sup>II</sup> complex is 6–10, whereas for **MRim<sub>4</sub>** (0.5 mM receptor, 20 mM DPC) it is even larger (i.e., 6–11). The fact that 50% acetylacetonate inclusion is detected at pH 5.8 indicates a pseudo-p*K*<sub>a</sub><sup>[32a]</sup> of 5.8, which corresponds to a shift of more than three units relative to free acetylacetone (p*K*<sub>a</sub> = 9).<sup>[32b]</sup> ITC measurements (Figure 6) gave corresponding *K'*<sub>acac</sub> values of 2.8(±0.7) × 10<sup>4</sup> M<sup>-1</sup> and 2.4(±0.7) × 10<sup>4</sup> M<sup>-1</sup> at pH 7 for **MRim<sub>4</sub>Zn<sup>II</sup>** and **WRim<sub>4</sub>Zn<sup>II</sup>**, respectively. Again, very similar thermodynamic parameters were found, indicating that in both cases the strong complexation is essentially enthalpy-driven ( $\Delta H^{\circ}$ <sub>acac</sub> = -23 ± 3 kJ mol<sup>-1</sup> and -24 ± 1 kJ mol<sup>-1</sup>,  $\Delta S^{\circ}$ <sub>acac</sub> = 8 ± 1 J K<sup>-1</sup> mol<sup>-1</sup> and 7 J K<sup>-1</sup> mol<sup>-1</sup>, for **MRim<sub>4</sub>Zn<sup>II</sup>** and **WRim<sub>4</sub>Zn<sup>II</sup>**, respectively).

### Acetamide

Having evidenced that the systems can bind acetylacetonate at neutral pH in spite of its high p*K*<sub>a</sub> value (9), acetamide coordination was studied, knowing that it is a poor ligand when neutral (especially in a competitive aqueous medium), but a strong donor when deprotonated. Coordination of acetamide by **WRim<sub>4</sub>Zn<sup>II</sup>** and **MRim<sub>4</sub>Zn<sup>II</sup>** was explored as a function of pD by <sup>1</sup>H NMR. The pD of a solution containing **WRim<sub>4</sub>** (1 mM), Zn<sup>II</sup> (2 mM), and acetamide (50 mM) was varied, and the NMR spectra showed the *endo* complexation of acetamide ( $\delta$  = -2.35 ppm for its methyl group) in the pD window 7.5–10.2, with an optimal pD of 9 for its inclusion. Titrations of **WRim<sub>4</sub>** and **MRim<sub>4</sub>** with acetamide at pD 8.4 allowed estimation of the corresponding *K'*<sub>MeCONH</sub> values as 400 and 700 M<sup>-1</sup>, respectively (Figures S22–S24). This is a remarkable result, considering the low hydrophobic driving force for such a small guest and its high p*K*<sub>a</sub> value (16).<sup>[33]</sup> The presence of about 50% of the *endo* complex at pD 7.5 indicates a pseudo p*K*<sub>a</sub> shift of eight units, which is impressive. Similar p*K*<sub>a</sub> shifts (ca. 8 units) have been

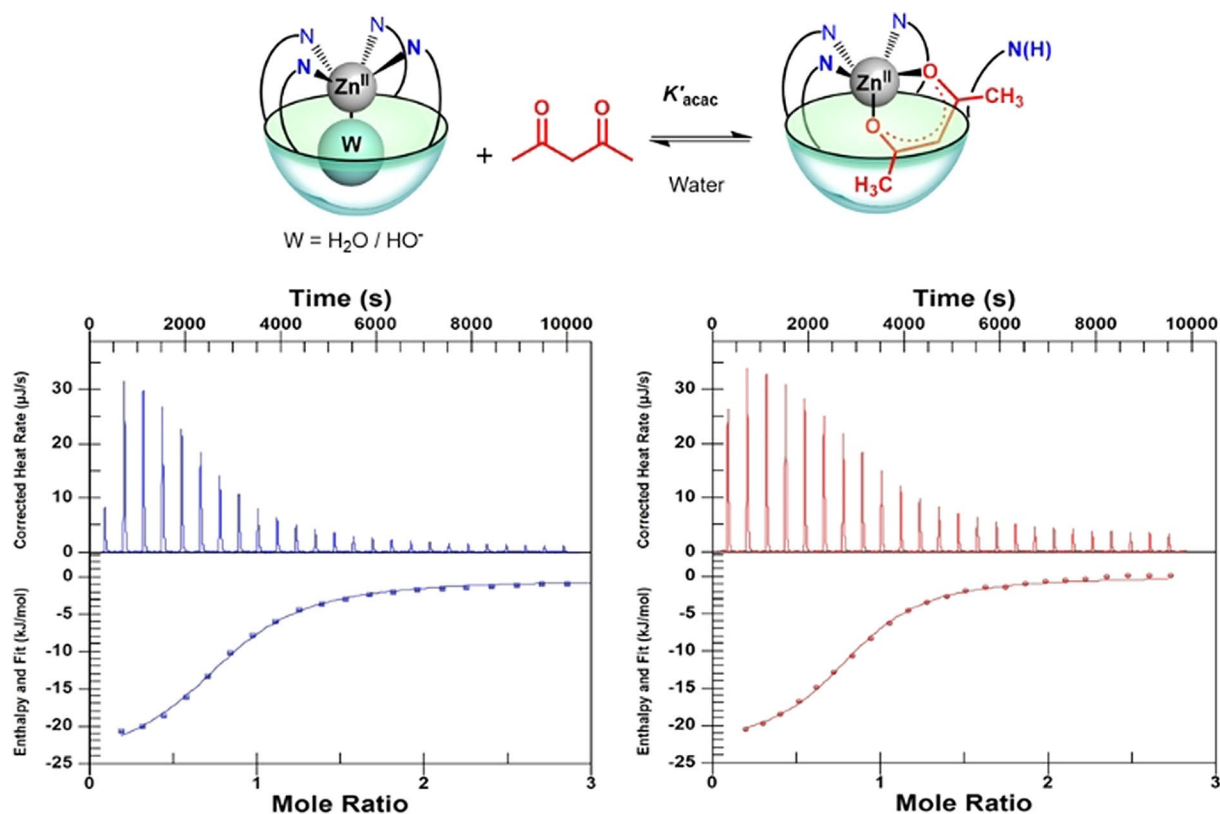


**Figure 6.** Complexation of acetylacetonate in water. The binding constant in micelles was obtained by ITC of **WRim<sub>4</sub>Zn<sup>II</sup>** (left, 0.8 mM) and **MRim<sub>4</sub>Zn<sup>II</sup>** (right, 0.5 mM, DPC 20 mM) with acetylacetonate at pH 7 (50 mM HEPES).

reported for acetamide residues that were intramolecularly coordinated to the metal center through a strong chelate effect with the formation of a five-membered ring.<sup>[34,35]</sup> In contrast, intermolecular coordination of amides (such as acetamide or benzamide) was not observed with these systems without a cavity. This shows that the stabilizing effect of the resorcinarene cavity on a guest has an impact that is as efficient as a strong chelate effect. Looking at the literature, we have not been able to find a comparable affinity for acetamide in water by any other molecular receptors.

## Conclusion

The water-soluble version of **Rim<sub>4</sub>**, namely **WRim<sub>4</sub>**, was successfully synthesized using the “feet” functionalization strategy. Indeed, the tetrapyrindinium salt, readily obtained from the hydroxylated precursor, was synthesized in eight steps from resorcinol, in an overall yield of 8%, as compared to five steps and 15% yield for its organosoluble analogue **Rim<sub>4</sub>**.<sup>[20]</sup> Water-solubilization of **Rim<sub>4</sub>** through its incorporation into DPC micelles was also successfully achieved. Both strategies led to mM concentrations of the ligand in water. Interestingly, the  $pK_a$  difference of 0.6 units for protonation of the ligand indicates that the micellar environment stabilizes the (partially) protonated form of **Rim<sub>4</sub>** more than water. This is probably indicative of stabilizing interactions of the cationic form by the phosphate moieties of the DPC micelles. This also accounts for the higher basic pH window (9.8 vs. 8.6) for coordination of the

**Zn<sup>II</sup>** cation. Importantly, both ligands **WRim<sub>4</sub>** and **MRim<sub>4</sub>** display good affinity for zinc, which they readily bind to give rise to a folded structure suitable for guest binding. In contrast to the enthalpy-driven coordination of **Zn<sup>II</sup>** by the organosoluble system **Rim<sub>4</sub>** in MeCN, it is entropy-driven in water, in which both systems **WRim<sub>4</sub>** and **MRim<sub>4</sub>** allow the stabilization of the bowl-shaped complexes over a wide pH window. The corresponding **Zn<sup>II</sup>** complexes bind small organic anions in water, at near-physiological pH, with efficiency and selectivity in spite of the hydrophilicity of the guests. Remarkably, they recognize acetamide as an anion at physiological pH in spite of its low acidity ( $pK_a$  16). The corresponding pseudo- $pK_a$  value of 7.5 equates to an impressive  $pK_a$  shift of 8.5, which is well explained by the establishment of a coordination bond with the Lewis acidic **Zn<sup>II</sup>** center concomitant with burial of the guest in the resorcinarene cavity. In comparison to simple **Zn<sup>II</sup>** complexes, the thermodynamic impact of the cavity for the stabilization of a metal-coordinated deprotonated amido moiety is as efficient as a five-membered ring chelate effect. To the best of our knowledge, this is the first example of a receptor capable of binding acetamide as an anion in water at physiological pH. As for the organosoluble version, the selectivity of guest hosting is cavity-driven by steric effects, with two coordination sites being available by virtue of the hemilability of one imidazole moiety. These hosting properties are in strong contrast to those displayed by calix[6]arene-based funnel complexes, which are excellent receptors for neutral guests such as amines, in spite of their protonated state at physiological pH,



but are unsuitable for anion binding due to second coordination sphere effects. This nicely illustrates the critical role of the architecture surrounding the coordination site of the metallo-receptor.

The study also gives new fundamental insights concerning the impact of a micellar environment, firstly for metal ion coordination, and secondly for guest hosting by a metallo-receptor comprising a cavity for binding, as in enzymes. Looking at the literature, we found no data on the metal coordination aspect. However, examples of metallo-probes directly incorporated into micelles show that the major effect of micelles on receptors lacking a cavity, beside their solubilization in aqueous media, is an enhanced affinity for lipophilic guests, which may be attributed to the hydrophobic effect.<sup>[24,36–39]</sup> The interesting case that we have highlighted is that of a uranyl-salophen complex embedded in cationic micelles,<sup>[23,40]</sup> which binds the highly hydrophilic fluoride anion with an increase in affinity of two orders of magnitude relative to the water-soluble version of the complex.<sup>[6]</sup> Electrostatic stabilization of the bound fluoride anion by the cationic micelle is probably a factor in accounting for this increased affinity.

As regards receptors presenting a cavity for guest hosting, only a few examples exploring the micellar effect with resorcinarene deep cavitands have been reported.<sup>[41,42]</sup> In these cases, an enhancement of guest binding was also observed (up to a factor of 180 in the presence vs. in the absence of DPC micelles in water), but its enthalpic origin indicated that it was related to a structural effect of the micellar environment that prevented dimerization of the receptor in the absence of the hydrophobic guest. The case study reported here addresses a different question, which is quite general and relevant to biological systems: what is the impact of the micellar environment on metal ion affinity and anionic guest hosting? In metallo-enzymes, the active site is generally surrounded by a hydrophobic environment provided by the proteic core, whereas water-solubility is ensured by a polar surface. Here, both systems **WRim<sub>4</sub>** and **MRim<sub>4</sub>** present the same rigid bowl-shaped hydrophobic cavity for guest hosting and the same first coordination sphere, with four imidazole arms pre-organized on the resorcinarene core for metal ion binding. In this study, we have compared the coordination properties in the highly polar water environment and the lipophilic environment provided by the DPC micelles. To our surprise, both systems proved to be equally efficient for Zn<sup>2+</sup> binding, with very similar enthalpic and entropic components. Likewise, comparison of the equilibria between the free state in water for small organic analytes (in anionic form for acetate, or neutral form for acetylacetone and acetamide) also shows similar *K* values. The similarity of the pH windows for both metal and guest binding is also surprising. Essentially the only difference that we observed was a slightly enlarged pH window (by 0.5–1 pH units) at basic pH values with micelles, which is reflected by the difference in the p*K<sub>a</sub>* values of the ligands **WRim<sub>4</sub>** and **MRim<sub>4</sub>**.

Also striking is the fact that the properties of **MRim<sub>4</sub>** (Zn<sup>II</sup> coordination and guest binding) more closely resemble those of **WRim<sub>4</sub>** than those of **Rim<sub>4</sub>** in MeCN. This can be attributed to the major role played by solvation of the free Zn<sup>II</sup> and free

guest as, once bound to the resorcinarene tris-imidazole structure, the metal and guest reside in an environment provided by the bowl-shaped Zn<sup>II</sup> complex, and this acts as an insulator with respect to the environment (DPC vs. water). In conclusion, this study has shown that both a water-solubilized **Rim<sub>4</sub>** derivative, **WRim<sub>4</sub>**, as well as its micelle-encapsulated equivalent, **MRim<sub>4</sub>**, behave as good ligands for Zn<sup>II</sup> binding in water, and the corresponding complexes serve as remarkable biomimetic receptors for small organic guests that bind as anions in spite of their intrinsic hydrophilicity. Our results also show that the zwitterionic DPC micelle, which mimics the hydrophobic proteic environment of metallo-enzyme active sites, has very little impact on metal ion affinity and guest hosting, provided that the biomimetic site is well structured and presents a pre-shaped receptor pocket. Hence, micellar incorporation of a lipophilic molecular receptor can be considered as an easy alternative to difficult synthetic work, as it does not disrupt its binding ability towards charged species (metal cations or anions). This represents a quite general approach that can be used with a wide variety of systems, thus opening new perspectives for molecular recognition in water, either for sensing, transport, or catalysis. We are currently exploring the hydrolytic reactivity of these complexes.

## Experimental Section

**General:** All solvents and reagents were purchased from suppliers and used without further purification. THF was distilled using a PureSolv PS-Micro Inert Technology purification system. NMR spectra were recorded with four spectrometers: a Varian 600 MHz, a Bruker UltraShield CryoProbe 500 MHz, a Bruker Avance 500 MHz, and a Bruker ARX 250 MHz, and chemical shifts ( $\delta$ ) are referred to SiMe<sub>4</sub>. Mass spectrometric (ESI-MS) analyses were performed on a Thermo-Finnigan LCQ Advantage spectrometer using methanol or water as solvent. IR spectra were recorded on a Perkin-Elmer Spectrum FTIR spectrometer equipped with a MIRacle™ single-reflection horizontal ATR unit. ITC experiments were conducted on a NanoITC calorimeter (TA Instruments) at 298 K. pD/pH measurements were performed with a Mettler-Toledo U402-M3-S7/200 long combination pH microelectrode. The indicated pD values refer to pH measured in D<sub>2</sub>O, with a correction of 0.4 pH units that allows comparison between these two notions, as previously reported.<sup>[43,44]</sup> Fits presented for 1:1 binding constants and p*K<sub>a</sub>* determination were obtained using Excel.

**Cavitand 3:** The tetrabromo cavitand **2** (2.52 g, 1.47 mmol) was thrice dissolved in dry THF and dried under vacuum for 1 h at 80 °C. The reagent was then dissolved in dry THF (25 mL) under argon. At –78 °C, 1.6 M *n*-butyllithium (11 mL, 15.4 mmol) was slowly added. After 1 h at –78 °C, paraformaldehyde (520 mg, 17.3 mmol) was added in one portion. The reaction medium was then agitated for 30 min at –78 °C. The flask was brought to RT, and the mixture was stirred overnight. The solvent was then evaporated and the residue obtained was partitioned between ethyl acetate (30 mL) and a saturated aqueous solution of NH<sub>4</sub>Cl (20 mL). The organic layer was then washed with brine (2 × 20 mL), dried over Na<sub>2</sub>SO<sub>4</sub>, and concentrated to dryness. The yellow crude product obtained was purified by flash chromatography on silica (CH<sub>2</sub>Cl<sub>2</sub>/EtOH, 9:1 to 8:2, v/v) to yield a white powder (1.00 g, 45%). *R<sub>f</sub>* = 0.12 (CH<sub>2</sub>Cl<sub>2</sub>/EtOH, 9:1); <sup>1</sup>H NMR (500 MHz, CDCl<sub>3</sub>, 300 K, TMS):  $\delta$  = 7.13 (s, 4H; H<sub>ar</sub>, down), 5.90 (d, <sup>3</sup>J(H,H) = 6.5 Hz, 4H; H<sub>out</sub>),

4.81 (t,  $^3J(\text{H,H})=8.0$  Hz, 4H;  $\text{CHCH}_2$ ), 4.55 (s, 8H;  $\text{Ar-CH}_2\text{-O}$ ), 4.42 (d,  $^3J(\text{H,H})=8.0$  Hz, 4H;  $\text{H}_{\text{in}}$ ), 3.76 (t,  $^3J(\text{H,H})=6.5$  Hz, 8H;  $\text{CH}_2\text{OTIPS}$ ), 2.28 (m, 8H;  $\text{CHCH}_2$ ), 1.59 (m, 8H;  $\text{CH}_2\text{CH}_2\text{CH}_2$ ), 1.07 ppm (s, 84H; TIPS);  $^{13}\text{C}$  NMR (150 MHz,  $\text{CDCl}_3$ , 300 K, TMS):  $\delta=153.8$  ( $\text{C}_{\text{Ar-O}}$ ), 138.3 ( $\text{C}_{\text{Ar-CH}}$ ), 126.6 ( $\text{C}_{\text{Ar-CH}_2\text{-OH}}$ ), 120.4 ( $\text{C}_{\text{Ar,down}}$ ), 99.9 ( $\text{C}_{\text{bridge}}$ ), 63.2 ( $\text{CH}_2\text{-OTIPS}$ ), 55.8 ( $\text{CH}_2\text{-OH}$ ), 36.6 ( $\text{CHCH}_2$ ), 31.2 ( $\text{CH}_2\text{CH}_2\text{CH}_2$ ), 26.4 ( $\text{CHCH}_2$ ), 18.3 ( $\text{Si-CH}(\text{CH}_3)_2$ ), 12.3 ppm ( $\text{Si-CH}$ ); IR:  $\tilde{\nu}=3365$ , 2942, 2865, 1587, 1461, 1385, 1298, 1245, 1107, 1019, 999, 962, 882, 726  $\text{cm}^{-1}$ .

**Cavitand 4:** The tetraalkylated cavitand **3** (810 mg, 0.53 mmol) was pre-dried by threefold sequential dissolution in distilled THF and evaporation of the solvent under argon, and finally dried under vacuum for 1 h at 80 °C. It was then dissolved in anhydrous DMF (8 mL) and the solution was slowly added to a solution of sodium hydride (60% dispersed in oil, 638 mg, 15.9 mmol, washed with pentane three times) in anhydrous DMF (7 mL, 0 °C). After 30 min, the mixture was brought back to RT and stirred for 2 h. At 0 °C, *N*-methylchloromethylimidazolium hydrochloride (710 mg, 4.24 mmol) was added in four portions at intervals of 15 min. After a further 15 min at 0 °C, the solution was allowed to warm to RT and stirred overnight under argon. Water (80 mL) was then added, and the precipitate formed was collected by filtration and washed with water (2 × 20 mL). The crude product (1.02 g) thus obtained was used without further purification in the following step.  $^1\text{H}$  NMR (500 MHz,  $\text{CDCl}_3$ , 300 K, TMS):  $\delta=7.05$  (s, 4H;  $\text{Ar-H}_{\text{down}}$ ), 6.93 (d,  $^3J(\text{H,H})=1.1$  Hz, 4H;  $\text{H}_{\text{im},\beta}$ ), 6.88 (d,  $^3J(\text{H,H})=1.1$  Hz, 4H;  $\text{H}_{\text{im},\alpha}$ ), 5.57 (d,  $^3J(\text{H,H})=7.0$  Hz, 4H;  $\text{O-CH}_2\text{-O}$ ), 4.73 (t,  $^3J(\text{H,H})=8.5$  Hz, 4H;  $-\text{CH}-$ ), 4.56 (s, 8H;  $\text{O-CH}_2\text{-Im}$ ), 4.20 (s, 8H;  $\text{Ar-CH}_2\text{-O}$ ), 4.16 (d,  $^3J(\text{H,H})=7.0$  Hz, 4H;  $\text{O-CH}_2\text{-O}$ ), 3.72 (t,  $^3J(\text{H,H})=6.5$  Hz, 8H;  $\text{CH}_2\text{-OTIPS}$ ), 3.61 (s, 12H;  $\text{N-CH}_3$ ), 2.22 (m, 8H;  $\text{CH-CH}_2$ ), 1.55 (m, 8H;  $\text{CH}_2\text{-CH}_2\text{-OTIPS}$ ), 1.06 ppm (m, 84H; TIPS);  $^{13}\text{C}$  NMR (150 MHz,  $\text{CDCl}_3$ , 300 K, TMS):  $\delta=154.0$  ( $\text{C}_{\text{Ar-O}}$ ), 144.4 ( $\text{C}_{\text{Ar-N}}$ ), 137.8 ( $\text{C}_{\text{Ar-CH}}$ ), 127.5 ( $\text{CH}_{\text{im},\beta}$ ), 123.6 ( $\text{C}_{\text{Ar-CH}_2\text{-O}}$ ), 122.1 ( $\text{CH}_{\text{im},\alpha}$ ), 120.6 ( $\text{CH}_{\text{Ar,down}}$ ), 99.4 ( $\text{O-CH}_2\text{-O}$ ), 64.7 ( $\text{O-CH}_2\text{-Im}$ ), 63.0 ( $\text{CH}_2\text{-OTIPS}$ ), 61.9 ( $\text{Ar-CH}_2\text{-O}$ ), 36.5 (CH), 32.9 ( $\text{CH}_2\text{-CH}_2\text{-OTIPS}$ ), 31.0 ( $\text{N-CH}_3$ ), 26.2 ( $\text{CH-CH}_2$ ), 18.1 ( $\text{Si-CH}_3$ ), 12.1 ppm ( $\text{Si-C}$ ); IR:  $\tilde{\nu}=3357$ , 2942, 2866, 1592, 1500, 1464, 1389, 1285, 1245, 1149, 1106, 1067, 1016, 969, 882, 745, 681  $\text{cm}^{-1}$ .

**Cavitand 5:** The tetraimidazole cavitand **4** (976 mg, 0.52 mmol) was dried under vacuum at 60 °C for 1 h. Under argon, it was dissolved in THF/ $\text{H}_2\text{O}$  (1:1, v/v, 54 mL), and then trifluoroacetic acid (7 mL) was slowly added. The mixture was stirred overnight at RT and then the solvent and TFA were evaporated. Toluene (3 mL) was thrice added and evaporated for better water elimination. The residue was dissolved in methanol (12 mL) and treated with a Dowex resin conditioned for  $\text{HO}^-$  exchange. After 1 h, the resin was filtered off and washed with methanol. The filtrate was concentrated to dryness. The yellowish solid obtained was purified by flash chromatography on silica ( $\text{MeOH}/\text{CH}_2\text{Cl}_2$ , 1:9 to 2:8, v/v, 0.3%  $\text{NH}_3$ ) to yield a yellow oil (627 mg, 93% over two steps).  $R_f=0.43$  ( $\text{MeOH}/\text{CH}_2\text{Cl}_2$ , 15:85, 0.3%  $\text{NH}_3$ );  $^1\text{H}$  NMR (500 MHz,  $\text{CD}_3\text{OD}$ , 300 K, TMS):  $\delta=7.33$  (s, 4H;  $\text{H}_{\text{Ar,down}}$ ); 7.31 (d,  $^3J(\text{H,H})=1.4$  Hz, 4H;  $\text{H}_{\text{in}}$ ); 7.21 (d,  $^3J(\text{H,H})=1.4$  Hz, 4H;  $\text{H}_{\text{im}}$ ), 5.71 (d,  $^3J(\text{H,H})=7.0$  Hz, 4H;  $\text{H}_{\text{out}}$ ), 4.69 (t,  $^3J(\text{H,H})=6.4$  Hz, 4H; CH), 4.67 (s, 8H;  $\text{O-CH}_2\text{-Im}$ ), 4.40 (s, 8H;  $\text{Ar-CH}_2\text{-O}$ ), 4.17 (d,  $^3J(\text{H,H})=7.0$  Hz, 4H;  $\text{H}_{\text{in}}$ ), 3.69 (s, 12H;  $\text{N-CH}_3$ ), 3.63 (t,  $^3J(\text{H,H})=6.5$  Hz, 8H;  $\text{CH}_2\text{OH}$ ), 2.32 (m, 8H;  $\text{CHCH}_2$ ), 1.47 ppm (m, 8H;  $\text{CH}_2\text{CH}_2\text{CH}_2$ );  $^{13}\text{C}$  NMR (150 MHz,  $\text{CD}_3\text{OD}$ , 300 K, TMS):  $\delta=155.7$  ( $\text{C}_{\text{Ar-O}}$ ), 145.6 ( $\text{C}_{\text{Ar-N}}$ ), 139.4 ( $\text{C}_{\text{Ar-CH}}$ ), 125.2 ( $\text{C}_{\text{Ar-C}_{\text{Ar-O}}}$ ), 124.6 ( $\text{C}_{\text{im},\alpha}$ ), 123.4 ( $\text{C}_{\text{Ar,down}}$ ), 121.5 ( $\text{C}_{\text{im},\beta}$ ), 101.4 ( $\text{C}_{\text{bridge}}$ ), 64.3 ( $\text{C}_{\text{Ar-CH}_2\text{-O}}$ ), 62.8 ( $\text{OCH}_2\text{Im}$ ), 62.6 ( $\text{CH}_2\text{OH}$ ), 38.3 ( $\text{CHCH}_2$ ), 34.7 ( $\text{N-CH}_3$ ), 32.1 ( $\text{CHCH}_2$ ), 27.4 ppm ( $\text{CH}_2\text{CH}_2\text{CH}_2$ ); IR:  $\tilde{\nu}=3357$ , 2922, 1633, 1567, 1501, 1470, 1411, 1285, 1243, 1140, 1063, 1019, 987, 747  $\text{cm}^{-1}$ ; HRMS:  $m/z$ : 1265.5743 [cavitand-H] $^+$  (calcd 1265.5770), 1287.2 [cavitand-Na] $^+$ , 633.5 [cavitand-2H] $^{2+}$ .

**WRim<sub>4</sub>:** Cavitand **5** (121 mg, 96  $\mu\text{mol}$ ) was dried by threefold dissolution in distilled THF (2 mL) and evaporation of the solvent under vacuum at 80 °C for 1 h. Under argon, the solid was dissolved in anhydrous pyridine (4.7 mL) and, at 0 °C, mesyl chloride (70  $\mu\text{L}$ , 1.1 mmol) was added. The reaction mixture was stirred overnight at RT, then heated at 100 °C for 24 h, whereupon a brown solid appeared. After cooling to RT, diethyl ether (5 mL) was added. The solution was filtered and the solid was washed with diethyl ether (2 × 5 mL). The crude product was dissolved in methanol (0.5 mL) and the solution was stirred for 1 h at RT with an ion-exchange resin for chlorides (Dowex). The resin was then collected by filtration and washed with methanol. The filtrate was concentrated to dryness to yield a brown solid (95 mg, 60%).  $^1\text{H}$  NMR (500 MHz,  $\text{CD}_3\text{OD}$ , 300 K, TMS):  $\delta=9.09$  (m, 8H; pyridine), 8.52 (m, 4H; pyridine), 8.06 (m, 8H; pyridine), 7.78 (s, 4H;  $\text{H}_{\text{Ar,down}}$ ), 6.97 (d,  $^3J(\text{H,H})=1.0$  Hz, 4H;  $\text{H}_{\text{im},\alpha}$ ), 6.79 (d,  $^3J(\text{H,H})=1.0$  Hz, 4H;  $\text{H}_{\text{im},\beta}$ ), 5.38 (d,  $^3J(\text{H,H})=7.5$  Hz, 4H;  $\text{H}_{\text{out}}$ ), 4.80 (m, 8H;  $\text{CH}_2\text{N}^+$ ), 4.57 (t,  $^3J(\text{H,H})=8.3$  Hz, 4H; CH), 4.36 (s, 8H;  $\text{O-CH}_2\text{-Im}$ ), 4.17 (s, 8H;  $\text{Ar-CH}_2\text{-O}$ ), 4.05 (d,  $^3J(\text{H,H})=7.5$  Hz, 4H;  $\text{H}_{\text{in}}$ ), 3.45 (s, 12H;  $\text{N-CH}_3$ ), 2.63 (m, 8H;  $\text{CHCH}_2$ ), 1.96 ppm (m, 8H;  $\text{CH}_2\text{CH}_2\text{CH}_2$ );  $^{13}\text{C}$  NMR (150 MHz,  $\text{CD}_3\text{OD}$ , 300 K, TMS):  $\delta=155.8$  ( $\text{C}_{\text{Ar-O}}$ ), 147.2 (pyridine), 146.3 (pyridine), 146.1 ( $\text{C}_{\text{Ar-N}}$ ), 138.9 ( $\text{C}_{\text{Ar-CH}}$ ), 129.8 (pyridine), 129.6 ( $\text{C}_{\text{Ar-C}_{\text{Ar-O}}}$ ), 127.5 ( $\text{C}_{\text{im},\alpha}$ ), 124.2 ( $\text{C}_{\text{Ar,down}}$ ), 124.0 ( $\text{C}_{\text{im},\beta}$ ), 101.4 ( $\text{C}_{\text{bridge}}$ ), 64.8 ( $\text{O-CH}_2\text{-C}_{\text{Ar-N}}$ ), 63.2 ( $\text{CH}_2\text{N}^+$ ,  $\text{C}_{\text{Ar-CH}_2\text{-O}}$ ), 38.4 (CH), 33.4 ( $\text{N-CH}_3$ ), 30.9 ( $\text{CHCH}_2$ ), 28.1 ppm ( $\text{CH}_2\text{CH}_2\text{CH}_2$ ); IR:  $\tilde{\nu}=3393$ , 2946, 1635, 1590, 1476, 1405, 1323, 1285, 1246, 1150, 1064, 1017, 966, 774, 686  $\text{cm}^{-1}$ ; HRMS:  $m/z$ : 378.1877 [cavitand] $^{4+}$  (calcd: 378.1818).

**[WRim<sub>4</sub>Zn]Cl<sub>4</sub>(NO<sub>3</sub>)<sub>2</sub>:** The zinc complex was generated in situ in  $\text{D}_2\text{O}$  by the addition of one equivalent of  $\text{Zn}(\text{NO}_3)_2$  to a solution of **WRim<sub>4</sub>**.  $^1\text{H}$  NMR (500 MHz,  $\text{D}_2\text{O}$ , pD 7.31, 300 K, TMS):  $\delta=8.91$  (m, 8H; pyridine), 8.60 (m, 4H; pyridine), 8.10 (m, 8H; pyridine), 7.59 (s, 4H;  $\text{H}_{\text{Ar,down}}$ ), 7.20 (s, 4H;  $\text{H}_{\text{im},\beta}$ ), 6.65 (brs, 4H;  $\text{H}_{\text{im},\alpha}$ ), 5.62 (d,  $^3J(\text{H,H})=7.0$  Hz, 4H;  $\text{H}_{\text{out}}$ ), 4.70 (s, 8H;  $\text{O-CH}_2\text{-Im}$ ), 4.49 (s, 8H;  $\text{Ar-CH}_2\text{-O}$ ), 4.28 (brs, 4H;  $\text{H}_{\text{in}}$ ), 3.76 (brs, 12H;  $\text{N-CH}_3$ ), 2.55 (m, 8H;  $\text{CHCH}_2$ ), 2.12 ppm (m, 8H;  $\text{CH}_2\text{CH}_2\text{CH}_2$ );  $^{13}\text{C}$  NMR (150 MHz,  $\text{D}_2\text{O}$ , pD 7.31, 300 K, TMS):  $\delta=153.6$  ( $\text{C}_{\text{Ar-O}}$ ), 145.8 (pyridine), 145.1 ( $\text{C}_{\text{Ar-N}}$ ), 144.1 (pyridine), 137.0 ( $\text{C}_{\text{Ar-CH}_{\text{Ar,down}}}$ ), 128.4 (pyridine), 125.3 ( $\text{C}_{\text{im},\alpha}$ ), 124.0 ( $\text{C}_{\text{im},\beta}$ ), 122.8 ( $\text{C}_{\text{Ar-C}_{\text{Ar-O}}}$ ), 122.4 ( $\text{CH}_{\text{Ar,down}}$ ), 100.0 ( $\text{C}_{\text{bridge}}$ ), 62.5 ( $\text{O-CH}_2\text{-Im}$ ), 61.7 ( $\text{Ar-CH}_2\text{-O}$ ), 61.5 ( $\text{CH}_2\text{N}^+$ ), 36.3 (CH), 33.3 ( $\text{N-CH}_3$ ), 28.9 ( $\text{CHCH}_2$ ), 26.1 ppm ( $\text{CHCH}_2\text{CH}_2$ ); IR:  $\tilde{\nu}=3430$ , 2935, 1642, 1563, 1349, 1245, 1152, 1048, 1024, 994, 968, 829, 765  $\text{cm}^{-1}$ .

**[MRim<sub>4</sub>Zn] $^{\text{II}}$ (ClO<sub>4</sub>)<sub>2</sub>:** From **MRim<sub>4</sub>**: The ligand **Rim<sub>4</sub>** (1.04 mg, 0.64  $\mu\text{mol}$ ), synthesized as reported previously,<sup>[20]</sup> was suspended in an acidic solution of DPC (10.7 mg, 20 mM, pD 2) in  $\text{D}_2\text{O}$  (for NMR studies;  $\text{H}_2\text{O}$  for ITC studies). The suspension was stirred at RT for 3 h, whereupon a clear solution was obtained, which was used as such for NMR or ITC studies. The corresponding zinc(II) complex **MRim<sub>4</sub>Zn** was generated by the addition of one equivalent of  $\text{Zn}(\text{ClO}_4)_2$ . **Direct synthesis of MRim<sub>4</sub>Zn**: The complex **[Rim<sub>4</sub>Zn(EtOH)](ClO<sub>4</sub>)<sub>2</sub>** (1.2 mg, 0.7  $\mu\text{mol}$ ), prepared as reported previously,<sup>[20]</sup> was suspended in HEPES buffer (1.47 mL, 50 mM, pD 7.4) containing DPC (10.3 mg, 20 mM). The suspension was stirred at RT overnight and then heated to 50 °C for 30 min. The limpid solution obtained was used as such for NMR studies.

**General NMR titration procedure:** Typically, **WRim<sub>4</sub>** (ca. 0.8 mg, 1 mM) or **MRim<sub>4</sub>Zn** (0.5 mM, DPC 20 mM) was dissolved in buffered  $\text{D}_2\text{O}$  (500  $\mu\text{L}$ ). The buffer was 100 mM HEPES (50 mM for micelles), adjusted to pD 7.4 with 1 M NaOH solution. When **WRim<sub>4</sub>** was used, an aliquot (5  $\mu\text{L}$ , 1 equiv) of a 0.1 M solution of  $\text{Zn}(\text{NO}_3)_2$  in  $\text{D}_2\text{O}$  was added. Aliquots (between 2 and 20  $\mu\text{L}$ ) of a solution of the guest (0.05 M, 10  $\mu\text{L}$  for 1 equiv) in the same buffer were progressively added until saturation and  $^1\text{H}$  NMR spectra were recorded.

ed after each addition. The final pD of the solution was measured to ensure that it remained constant during the whole experiment.

**General ITC procedure:** An aliquot (1 mL) of host solution was introduced into the cell of the calorimeter. The titrant solution was added by means of a 250  $\mu\text{L}$  syringe in 24 injections of 10  $\mu\text{L}$  at intervals of 400 s. A blank was recorded by replacing the solution in the cell with 1 mL of solvent. The obtained data were processed with Nanoanalyze software.

## Acknowledgements

This project was supported by the CNRS and the Ministère de l'Enseignement Supérieur et de la Recherche. The authors also acknowledge the FRIA-FRS (Ph.D. grant to E.B.), the FNRS, and the Van Buuren foundation for funding of the ITC equipment. This article is published with the help of the Fondation Universitaire de Belgique.

## Conflict of interest

The authors declare no conflict of interest.

**Keywords:** biomimetism · micelles · resorcinarene · water-soluble · zinc

- [1] E. A. Kataev, C. Müller, *Tetrahedron* **2014**, *70*, 137–167.
- [2] P. S. Cremer, A. H. Flood, B. C. Gibb, D. L. Mobley, *Nat. Chem.* **2017**, *10*, 8–16.
- [3] F. Biedermann, W. M. Nau, H.-J. Schneider, *Angew. Chem. Int. Ed.* **2014**, *53*, 11158–11171; *Angew. Chem.* **2014**, *126*, 11338–11352.
- [4] P. Sokkalingam, J. Shraberg, S. W. Rick, B. C. Gibb, *J. Am. Chem. Soc.* **2016**, *138*, 48–51.
- [5] J. Murray, K. Kim, T. Ogoshi, W. Yao, B. C. Gibb, *Chem. Soc. Rev.* **2017**, *46*, 2479–2496.
- [6] M. J. Langton, C. J. Serpell, P. D. Beer, *Angew. Chem. Int. Ed.* **2016**, *55*, 1974–1987; *Angew. Chem.* **2016**, *128*, 2012–2026.
- [7] S. Kubik, *Acc. Chem. Res.* **2017**, *50*, 2870–2878.
- [8] A. Dalla Cort, G. Forte, L. Schiaffino, *J. Org. Chem.* **2011**, *76*, 7569–7572.
- [9] H. T. Ngo, X. Liu, K. A. Jolliffe, *Chem. Soc. Rev.* **2012**, *41*, 4928–4965.
- [10] S. J. Butler, D. Parker, *Chem. Soc. Rev.* **2013**, *42*, 1652–1666.
- [11] O. Bistri, O. Reinaud, *Org. Biomol. Chem.* **2015**, *13*, 2849–2865.
- [12] J. M. Fox, K. Kang, W. Sherman, A. Héroux, G. M. Sastry, M. Baghbanzadeh, M. R. Lockett, G. M. Whitesides, *J. Am. Chem. Soc.* **2015**, *137*, 3859–3866.
- [13] J.-N. Rebilly, O. Reinaud, *Supramol. Chem.* **2014**, *26*, 454–479.
- [14] O. Sénèque, M.-N. Rager, M. Giorgi, O. Reinaud, *J. Am. Chem. Soc.* **2000**, *122*, 6183–6189.
- [15] D. Coquière, S. Le Gac, U. Darbost, O. Sénèque, I. Jabin, O. Reinaud, *Org. Biomol. Chem.* **2009**, *7*, 2485–2500.
- [16] J.-N. Rebilly, B. Colasson, O. Bistri, D. Over, O. Reinaud, *Chem. Soc. Rev.* **2015**, *44*, 467–489.
- [17] N. Le Poul, Y. Le Mest, I. Jabin, O. Reinaud, *Acc. Chem. Res.* **2015**, *48*, 2097–2106.
- [18] G. Izzet, X. Zeng, H. Akdas, J. Marrot, O. Reinaud, *Chem. Commun.* **2007**, 810–812.
- [19] J. Gout, S. Rat, O. Bistri, O. Reinaud, *Eur. J. Inorg. Chem.* **2014**, 2819–2828.
- [20] A. Parrot, S. Collin, G. Bruylants, O. Reinaud, *Chem. Sci.* **2018**, *9*, 5479–5487.
- [21] O. Bistri, B. Colasson, O. Reinaud, *Chem. Sci.* **2012**, *3*, 811–818.
- [22] A. Inthasot, N. Le Poul, M. Luhmer, B. Colasson, I. Jabin, O. Reinaud, *Inorg. Chem.* **2018**, *57*, 3646–3655.
- [23] M. Cametti, A. Dalla Cort, K. Bartik, *ChemPhysChem* **2008**, *9*, 2168–2171.
- [24] F. Su, R. Alam, Q. Mei, Y. Tian, C. Youngbull, R. H. Johnson, D. R. Meldrum, *PLoS ONE* **2012**, *7*, e33390.
- [25] E. Brunetti, A. Inthasot, F. Keymeulen, O. Reinaud, I. Jabin, K. Bartik, *Org. Biomol. Chem.* **2015**, *13*, 2931–2938.
- [26] A. Višnjevac, J. Gout, N. Ingert, O. Bistri, O. Reinaud, *Org. Lett.* **2010**, *12*, 2044–2047.
- [27] S. Rat, J. Gout, O. Bistri, O. Reinaud, *Org. Biomol. Chem.* **2015**, *13*, 3194–3197.
- [28] K.-D. Zhang, D. Ajami, J. Rebek, *J. Am. Chem. Soc.* **2013**, *135*, 18064–18066.
- [29] B. C. Gibb, R. G. Chapman, J. C. Sherman, *J. Org. Chem.* **1996**, *61*, 1505–1509.
- [30] U. Darbost, M.-N. Rager, S. Petit, I. Jabin, O. Reinaud, *J. Am. Chem. Soc.* **2005**, *127*, 8517–8525.
- [31] S. J. Hawkes, *J. Chem. Educ.* **1996**, *73*, 516–517.
- [32] a) The pseudo  $pK_a$  value associated with the guest molecule ( $\text{GH}/\text{G}^-$ ) is defined by the following equilibrium:  $\text{Rim}_4\text{Zn}^{2+} + \text{GH} \rightleftharpoons \text{Rim}_4\text{Zn}(\text{G})^+ + \text{H}^+$ . In the case of acetylacetone, however, it is not clear whether the Acac decoordination at low pH is due to its protonation or to protonation of the  $\text{Rim}_4$  ligand; b) R. G. Pearson, R. L. Dillon, *J. Am. Chem. Soc.* **1953**, *75*, 2439–2443.
- [33] F. G. Bordwell, *Acc. Chem. Res.* **1988**, *21*, 456–463.
- [34] For the coordination of  $\alpha$ -amino-acetamide to  $\text{Cu}^{\text{II}}$ , a pseudo- $pK_a$  of 8.0 was reported. P. M. H. Kroneck, V. Vortisch, P. Hemmerich, *Eur. J. Biochem.* **1980**, *109*, 603–612.
- [35] For the coordination of an acetamido moiety grafted on a cyclen ligand, a pseudo- $pK_a$  of 7.9 was reported for the corresponding  $\text{Zn}^{\text{II}}$  complex. E. Kimura, T. Gotoh, S. Aoki, M. Shiro, *Inorg. Chem.* **2002**, *41*, 3239–3248.
- [36] F. Mancin, P. Scrimin, P. Tecilla, U. Tonellato, *Coord. Chem. Rev.* **2009**, *253*, 2150–2165.
- [37] P. Pallavicini, Y. A. Diaz-Fernandez, L. Pasotti, *Coord. Chem. Rev.* **2009**, *253*, 2226–2240.
- [38] P. Grandini, F. Mancin, P. Tecilla, P. Scrimin, U. Tonellato, *Angew. Chem. Int. Ed.* **1999**, *38*, 3061–3064; *Angew. Chem.* **1999**, *111*, 3247–3250.
- [39] T. Riis-Johannessen, K. Severin, *Chem. Eur. J.* **2010**, *16*, 8291–8295.
- [40] F. Keymeulen, P. De Bernardin, A. Dalla Cort, K. Bartik, *J. Phys. Chem. B* **2013**, *117*, 11654–11659.
- [41] Y. J. Kim, M. T. Lek, M. P. Schramm, *Chem. Commun.* **2011**, *47*, 9636–9638.
- [42] S. Javor, J. Rebek, *J. Am. Chem. Soc.* **2011**, *133*, 17473–17478.
- [43] P. K. Glasoe, F. A. Long, *J. Phys. Chem.* **1960**, *64*, 188–190.
- [44] K. Mikkelsen, S. O. Nielsen, *J. Phys. Chem.* **1960**, *64*, 632–637.

Manuscript received: September 18, 2018  
Revised manuscript received: October 16, 2018  
Accepted manuscript online: October 17, 2018  
Version of record online: November 26, 2018